Blockade of EGFR and ErbB2 by the Novel Dual EGFR and ErbB2 Tyrosine Kinase Inhibitor GW572016 Sensitizes Human Colon Carcinoma GEO Cells to Apoptosis

Yunfei Zhou,[1] Song Li,[2] Yi P. Hu,[1] Jing Wang,[1] Jennie Hauser,[1] Alexis N. Conway,[1] Michelle A. Vinci,[1] Lisa Humphrey,[1] Elizabeth Zborowska,[3] James K.V. Willson,[3] and Michael G. Brattain[1]

Departments of [1]Pharmacology and Therapeutics and [2]Chemoprevention, Roswell Park Cancer Institute, Buffalo, New York and [3]Department of Medicine, Ireland Cancer Center, Case Western Reserve University, Cleveland, Ohio

Abstract

Coexpression of the epidermal growth factor receptor (EGFR) family receptors is found in a subset of colon cancers, which may cooperatively promote cancer cell growth and survival, as heterodimerization is known to provide for diversification of signal transduction. Recently, efforts have been made to develop novel 4-anilinoquinazoline and pyridopyrimidine derivatives to inhibit EGFR and ErbB2 kinases simultaneously. In this study, we tested the efficacy of a novel reversible dual inhibitor GW572016 compared with the selective EGFR and ErbB2 tyrosine kinase inhibitors (TKI) AG1478 and AG879 and their combination, using the human colon adenocarcinoma GEO mode. GEO cells depend on multiple ErbB receptors for aberrant growth. A synergistic effect on inhibition of cell proliferation associated with induction of apoptosis was observed from the combination of AG1478 and AG879. Compared with AG1478 or AG879, the single TKI compound GW572016 was a more potent inhibitor of GEO cell proliferation and was able to induce apoptosis at lower concentrations. Western blot analysis revealed that AG1478 and AG879 were unable to suppress both EGFR and ErbB2 activation as well as the downstream mitogen-activated protein kinase (MAPK) and AKT pathways as single agents. In contrast, GW572016 suppressed the activation of EGFR, ErbB2, MAPK, and AKT in a concentration-dependent manner. Finally, *in vivo* studies showed that GW572016 treatment efficiently blocked GEO xenograft growth at a dose range of 30 to 200 mg/kg with a twice-daily schedule. In summary, our study indicates that targeting both EGFR and ErbB2 simultaneously could enhance therapy over that of single agents directed at EGFR or ErbB2 in cancers that can be identified as being primarily heterodimer-dependent. (Cancer Res 2006; 66(1): 404-11)

Introduction

The ErbB receptor family, which includes epidermal growth factor receptor (EGFR; ErbB1/HER1), ErbB2/neu/HER2, ErbB3/HER3, and ErbB4/HER4, is widely expressed in epithelial, mesenchymal, and neuronal tissues, where the receptors play pivotal roles in a variety of critical cellular functions (1, 2). Members of the family have been shown to be oncogenic. Overexpression of wild-type EGFR or ErbB2 or expression of constitutively activated receptor mutants transforms cells *in vitro* (3–5). ErbB receptor signals through a network involving receptor homodimerization or heterodimerization. Cooperation between ErbB receptors has been observed in oncogenic transformation in cell culture (6). Briefly, the transforming effects of ErbB receptors are mediated through two major pathways. One is the well-characterized Ras/Raf/MAP kinase (MAPK) pathway that promotes DNA synthesis and cell cycle progression (7). Another pathway is activated through phosphoinositol 3-kinase (PI3K), which subsequently activates AKT, well known for its antiapoptotic properties and enhancement of cell survival (8–10).

Clinically, overexpression of EGFR has been implicated in the development and progression of head and neck, lung, pancreas, bladder, and breast cancer (11). High ErbB2 expression levels correlate with poor prognosis in cancers of the colon, ovary, breast, and bladder (12–14). ErbB3 is also widely expressed in several types of carcinomas, including colon cancer (15). Besides overexpression of the receptors, hyperactivation of the ErbB network can occur via autocrine loops involving inappropriate expression of the ErbB ligands by the tumor cells (16). Several investigations have shown that amphiregulin, CRIPTO, transforming growth factor α (TGFα), and heregulin expression led to aberrant ErbB activation in the absence of receptor overexpression (17–20). Accumulating evidence suggests that ErbB receptors are constitutively activated during growth factor and nutrient deprivation stress in colon carcinoma cells through autocrine activity (17, 21, 22). This autocrine activity has been shown to support malignant behavior of colon cancer cells (23). Furthermore, stable transfection of TGFα converts nonaggressive colon cancer cells to aggressive phenotypes that signal through EGFR/ErbB2 heterodimers without significant enhancement of receptor expression (18, 24, 25).

The GEO human colon carcinoma cell line has been widely used for testing anti-ErbB therapies, including antisense approaches to ErbB ligands and receptors, monoclonal antibodies, and small molecule tyrosine kinase inhibitors (TKI) with or without other chemotherapies (26–30). GEO cells express EGFR, ErbB2, and ErbB3 receptors at relatively "normal" levels but do not express ErbB4 (17, 24, 26). Multiple EGFR ligands are expressed in GEO cells, including amphiregulin, CRIPTO, and TGFα (31). It has been observed that antisense oligonucleotide approaches targeting individual ligands resulted in equipotent inhibition of cell proliferation in GEO cells (31, 32). However, in growth factor–deprived states, the EGFR autocrine activity is quenched due to down-regulation of ligand expression. Heregulin-stimulated ErbB2/ErbB3 heterodimer signaling plays a primary

Requests for reprints: Michael G. Brattain, Department of Molecular Pharmacology and Cancer Therapeutics, Elm and Carlton Streets, Buffalo, NY 14263. Phone: 716-845-3044; Fax: 716-845-4437; E-mail: Michael.brattain@roswellpark.org.

doi:10.1158/0008-5472.CAN-05-2506

role in sustaining GEO cell survival during growth factor deprivation as shown by heregulin-neutralizing antibody-mediated apoptosis in GEO cells (17). ErbB2 knockdown reduced tumorigenicity of the cells in conjunction with increased sensitivity to apoptosis by growth factor deprivation (25).

The synergistic transforming effects of EGFR and ErbB2 and the use of multiple ErbB receptors for cell proliferation and survival in tumor cells lead to the hypothesis that targeting both the EGFR and ErbB2 catalytic domains simultaneously would have superior therapeutic effects relative to single-agent treatment for tumors relying on both receptors. EGFR and ErbB2 have the highest homology among the EGFR family members in their kinase catalytic domains and share many similar biochemical and kinetic properties (33). Recently, efforts have been made to develop 4-anilinoquinazoline and pyridopyrimidine derivative dual inhibitors toward both EGFR and ErbB2 ATP-binding domains (34–36). GW572016 is a novel dual inhibitor, which reversibly inhibits the tyrosine kinase activities of both EGFR and ErbB2 at equal potency (37). We have tested the efficacy of GW572016 and single EGFR and ErbB2 TKIs AG1478 and AG879, respectively, using the GEO colon carcinoma model in this study. We observed a synergistic effect on inhibition of cell proliferation as well as induction of apoptosis from the combination of AG1478 and AG879, suggesting that both EGFR and ErbB2 activation were required for GEO cell proliferation and survival. In comparison, the single TKI compound GW572016 was more potent for inhibiting GEO cell proliferation than AG1478 and AG879 and was able to induce apoptosis at lower concentrations as reflected by poly(ADP-ribose) polymerase (PARP) cleavage and DNA fragmentation. Western blot analysis revealed that AG1478 and AG879 single agents were unable to suppress EGFR and ErbB2 activation as well as the MAPK and AKT downstream pathways. In contrast, GW572016 suppressed activation of EGFR, ErbB2, and the MAPK and AKT downstream pathways. Finally, *in vivo* studies showed that GW572016 treatment blocked GEO xenograft growth in a concentration-dependent manner. In summary, our study implied that targeting both EGFR and ErbB2 simultaneously with small molecule inhibitors, such as GW572016, is a valid strategy for colon cancer therapy.

Materials and Methods

Cell culture. The GEO cells were originally isolated from a primary human colon carcinoma, and its *in vitro* properties have been extensively characterized (38). Cells were maintained at 37°C in a humidified atmosphere of 6% CO_2 and grown continuously in a chemically defined McCoy'5A (Cellgro, Herndon, VA) serum-free medium supplemented with pyruvate, vitamins, amino acids, and antibiotics, plus EGF (10 ng/mL; R&D systems, Minneapolis, MN), insulin (20 μg/mL; Sigma, St. Louis, MO), and transferrin (4 μg/mL; Sigma). Supplemented medium is the basal medium lacking transferrin, insulin, and EGF. GEO cells at 90% confluent level (subconfluent) were deprived of exogenous growth factors by changing them to supplemented medium for 5 days. This is sufficient to drive the cells into a state of quiescence (G_0).

Drugs and antibodies. The selective EGFR TKI AG1478 and the selective ErbB2 TKI AG879 were purchased from Calbiochem (La Jolla, CA). The dual inhibitor GW572016 was provided by GlaxoSmithKline Pharmaceuticals (Research Triangle Park, NC). AG1478, AG879, and GW572016 were dissolved in DMSO (Sigma) for preparation of 20 or 10 mmol/L stock solutions. Drug solutions for treatment were serially diluted with serum-free medium from the stock solutions. A mixture of AG1478 and AG879 was prepared at a fixed ratio of 10:1 and serially diluted to working concentrations for the combination studies. An equivalent serial dilution of DMSO was used as control treatment.

The polyclonal antibodies for total EGFR, ErbB2, MAPK, and monoclonal antibodies for PARP and phospho-MAPK were purchased from Santa Cruz Biotechnology (Santa Cruz, CA). The monoclonal antibody specific to EGFR phosphotyrosine Y1173 was purchased from Calbiochem. The polyclonal antibody to ErbB2 phosphotyrosine Y1248 was purchased from Upstate Biotechnology (Lake Placid, NY). The polyclonal antibodies for phospho-AKT Ser^{473} and total AKT were purchased from Cell Signaling Technology (Beverly, MA). Blocking buffer and working concentrations of the above antibodies were prepared according to the data sheets of the products.

Cell growth inhibition assay. Inhibition of cell proliferation was evaluated by 3-(4,5-dimethylthiazol-2-yl)-2,5-diphenyltetrazolium bromide (MTT; Sigma). Briefly, cells were seeded in 96-well tissue culture plates (Costar, Corning, NY) at a density of 3,000 per 100 μL/well. Eight wells were assigned to each experimental treatment. After attachment for 24 hours, cells were treated with serial concentrations of AG1478, AG879, GW572016 or the combinations of AG1478 + AG879 as indicated in the relevant figures. After 72 hours of drug exposure, 100 μL of MTT solution (2 mg/mL) were added to each well for 2 hours of incubation. The reaction was stopped by removal of MTT, and formazan crystals were solubilized in 200 μL DMSO in each well. Absorbance at 570 nm was recorded using a 96-well microplate reader (ELx-808, Cambrex, Baltimore, MD).

Analysis of combination index. Synergistic effects between AG1478 and AG879 were analyzed using the combination index described by Chou and Talalay (39). A combination index of 1 indicates an additive effect between two drugs. Synergism is reflected by combination index of <1. Antagonism is reflected by combination index of >1. Combination index values were analyzed using the Calcusyn software (Biosoft, Ferguson, MO). The inputs are the concentrations of drug treatments and fractional inhibition (fraction affected or F_a). F_a was evaluated by MTT assay and calculated through the formula: $F_a = 1 - A_{570\ \text{treated}} / A_{570\ \text{control}}$.

DNA fragmentation assay (Cell Death Detection ELISA). Apoptosis was quantified by a DNA fragmentation ELISA. Briefly, cells were seeded in 96-well plates in serum-free medium at a density of 10,000 per 150 μL/well and allowed to attach for 24 hours. The next day, cells were treated with single TKIs or combinations at 37°C for up to 72 hours. DMSO was used as a control. DNA fragmentation was detected by the Cell Death Detection ELISA Plus kit (Roche, Indianapolis, IN) according to the manufacturer's instructions. Fold increases of DNA fragmentation were normalized with MTT readings from identical treatment conditions.

Western blot analysis. Cells were washed twice with cold PBS and then lysed with 300 μL TNESV lysis buffer containing 50 mmol/L Tris (pH 7.5), 150 mmol/L NaCl, 1% NP40, 50 mmol/L NaF, 1 mmol/L Na_3VO_4, 25 μg/mL β-glycerophosphate, 1 mmol/L phenylmethylsulfonyl fluoride, and one protease inhibitor cocktail tablet (Roche) per 10 mL for 30 minutes on ice. Protein estimation was determined by the Bio-Rad (Hercules, CA) method. After resolving the proteins on the SDS-PAGE, proteins were transferred to polyvinylidene difluoride membranes (Amersham Pharmacia Biotech, Arlington Heights, IL). The membranes were blocked with 5% nonfat dry milk in TBS/Tween 20 (TTBS) containing 0.15 mol/L NaCl, 0.01 mol/L Tris-HCl (pH 7.4), and 0.05% Tween 20 at room temperature for an hour. Primary antibodies at the manufacturer's recommended dilutions were incubated overnight at 4°C in 5% TTBS or 5% bovine serum albumin. After washing, blots were then incubated with a 1:5,000 dilution of horseradish peroxidase–linked secondary antibody at room temperature for 1 hour followed by further washing. Enhanced chemiluminescence was done according to the manufacturer's instructions (Amersham Biosciences, Little Chalfont, Buckinghamshire, United Kingdom).

Xenograft tumorigenicity studies. A total volume of 0.2 mL GEO cell suspension containing 5×10^6 cells was injected into both hind limbs of BALB/c athymic nude mice. Tumors became readily apparent after 7 days. Starting from day 8 to day 28, mice received oral administrations of GW572016 at 30, 100, and 200 mg/kg twice daily by oral gavage. The control group mice received 0.5% hydroxypropylmethylcellulose and 0.1% Tween 80 vehicle treatment. Each treatment group was represented by eight tumor

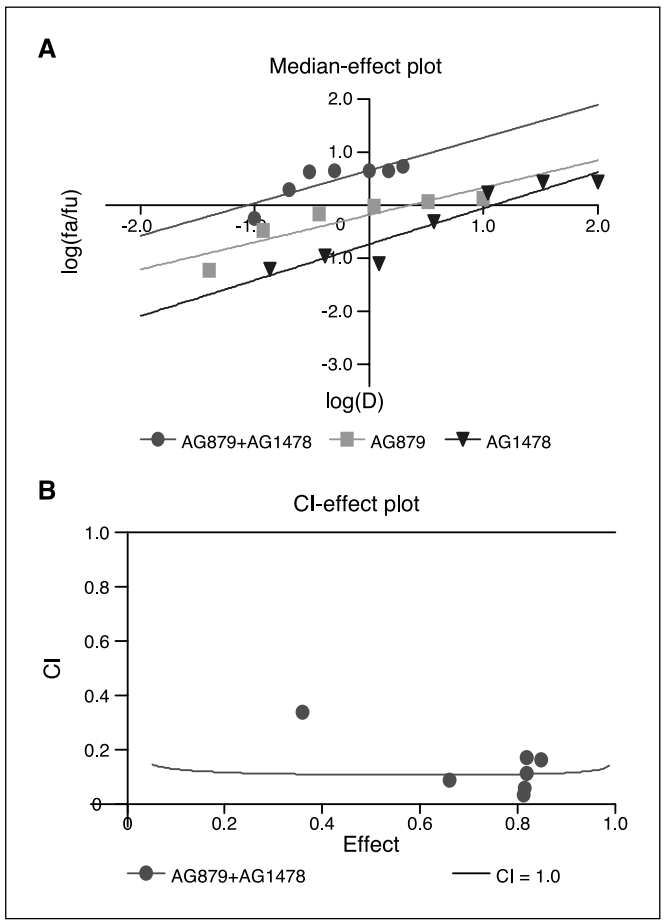

Figure 1. Synergistic effect of AG1478 and AG879 on growth inhibition in GEO cells. *A,* median-effect plot. Effect of AG1478, AG879, or AG1478 + AG879 at a 10:1 ratio was measured by MTT assay as described in Materials and Methods. The log values of the ratios of fraction affected to fraction unaffected [$\log(F_a/F_u)$] were plotted against log values of concentrations of AG1478 and AG879 single agents or AG879 concentrations in combinations as shown in the median-effect plot. IC_{50} values of single drugs or the combination was determined from the *x*-intercepts where $\log(F_a/F_u) = 0$. *B,* combination index (*CI*)/effect plot. Combination index values of combination treatment were analyzed by Calcusyn software (Biosoft) and plotted against fractional inhibition by the combination treatment. Strong synergism (combination index < 0.3) was indicated for AG1478 and AG879 at all combination concentrations tested. Similar experiments were repeated twice. Representative data.

xenografts. Tumor volume for xenografts was determined by externally measuring the tumors in two dimensions using a caliper. Volume (V) was determined by the following equation, where L is length and W is width of the tumor: $V = (L \times W^2) \times 0.5$.

Results

Synergistic effects on GEO cell growth inhibition by the combination of EGFR and ErbB2 TKIs. The EGFR kinase inhibitor AG1478 has four orders of magnitude higher selectivity to EGFR (IC_{50} = 3 nmol/L) than ErbB2 (IC_{50} >100 μmol/L) in cell-free systems. The ErbB2 kinase inhibitor AG879 has at least 500-fold higher selectivity to ErbB2 (IC_{50} = 1 μmol/L) than EGFR (IC_{50} >500 μmol/L) in cell-free systems (40). We first examined the growth inhibitory effects of AG1478 and AG879 in GEO cells by MTT assay. Drug concentrations and growth inhibitory effects were analyzed by Calcusyn software (Biosoft) and visualized as median-effect plots (Fig. 1*A*), which show the linear relationship between drug concentrations and the ratios of fraction affected (F_a) to fraction unaffected (F_u), where $F_u = 1 - F_a$ in log values. A concentration-dependent inhibition of cell proliferation was observed in both AG1478 and AG879 treatment alone with IC_{50} values at 10 and 2 μmol/L, respectively, as shown in Table 1. The IC_{50} values of drugs were determined from the *x*-intercept of the median-effect plots. A combination of AG1478 + AG879 at a fixed ratio of 10:1 was tested in parallel. The concentrations of AG879 tested in the combination were 2, 1.5, 1, 0.75, 0.5, 0.3, 0.15, and 0.1 μmol/L (1, 0.76, 0.5, 0.375, 0.25, 0.15, 0.075, 0.05 of the IC_{50} of AG879, respectively), whereas the concentrations of AG1478 were correspondingly 10-fold higher. Combination treatment resulted in a dramatic shift to the left of the median-effect plot, indicating higher potency of the combination treatment for inhibition of GEO cell proliferation. Correspondingly, the concentrations of AG1478 and AG879 were both reduced dramatically for induction of 50% growth inhibition used as a combination relative to the single agents (Table 1). By analyzing combination index values of AG1478 + AG879, a strong synergistic effect (combination index < 0.3) was determined at all combination concentrations tested (Fig. 1*B*).

Effects of AG1478 + AG879 on modification of EGFR, ErbB2, and the downstream MAPK and AKT pathways. It was previously found that the growth-arrested GEO cells generated constitutive activation of ErbB2 through a robust autocrine heregulin/ErbB3 loop, and the deregulated ErbB2/ErbB3 activation in GEO cells resulted in constitutive activation of the MAPK and PI3K/AKT pathways (17, 41). Consequently, we tested the effect of AG1478 and AG879 as single agents or in combination on EGFR and ErbB2 phosphorylation and the downstream MAPK and AKT pathways (Fig. 2). As shown in Fig. 2*A*, activation of EGFR and ErbB2 were both detectable in quiescent GEO cells. The EGFR-selective TKI AG1478 was sufficient to block phosphorylation of the EGFR Y1173 site at 5 μmol/L. However, this concentration of AG1478 failed to inhibit phosphorylation of the ErbB2 Y1248 site. Similarly, the ErbB2-selective TKI AG879 blocked activation of the ErbB2 Y1248 site at 1 μmol/L; however, it failed to inhibit EGFR activation. In contrast, the combination of AG1478 and AG879 at the same concentrations used in single-drug treatment inhibited both EGFR and ErbB2 phosphorylation. Interestingly, AG879 treatment resulted in an up-regulation of phosphorylation at the EGFR Y1173 site, which was consistent with our previous observation that inhibition of ErbB2 in these cells results in an

Table 1. IC_{50} values of AG1478, AG879, AG1478 + AG879, and GW572016 in GEO cell*

Drug treatment	IC_{50} value (μmol/L)
AG1478 single agent	10.37 ± 0.37
AG879 single agent	1.84 ± 0.18
AG1478+AG879(10:1 ratio) †	
AG879	0.83
AG1478	0.08
GW572016 single agent	0.3 ± 0.017

NOTE: The experiment was repeated twice, and representative data was shown here.
*IC_{50} values listed in the table are calculated from MTT data by Calcusyn software.
†IC_{50} values were generated from Fig. 1*A*.

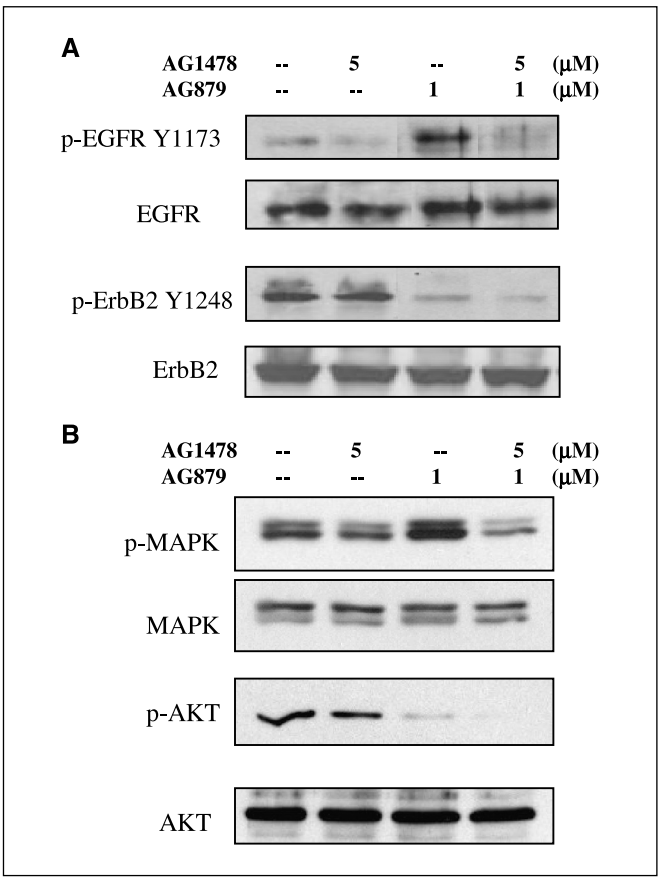

Figure 2. Effect of AG1478 + AG879 on EGFR, ErbB2, MAPK, and AKT. Subconfluent GEO cells were deprived of growth factors for 5 days to induce a quiescent state. Cells were pretreated with AG1478, AG879, and AG1478 + AG879 at the indicated concentrations for 6 hours. Cells were then released in fresh supplemented medium containing DMSO (0.1%) or different concentrations of drugs as indicated for 24 hours. Whole cell lysates were subjected to SDS PAGE analysis and probed with specific anti-phospho-antibodies against EGFR Y1173 and ErbB2 Y1248 (*A*) or MAPK and AKT (*B*). Total EGFR, ErbB2, or total MAPK and AKT were used as loading controls. Similar experiments were repeated at least twice. Representative data.

compensatory increase of EGFR and its constitutive activation (25). In Fig. 2*B*, single agent AG1478 showed a moderate inhibitory effect on both MAPK and a smaller effect on AKT activation. In contrast, single agent AG879 efficiently inhibited AKT activation, whereas a compensatory activation of MAPK was detected in conjunction with the increased EGFR activation during ErbB2 TKI treatment, arguing that the up-regulated EGFR activation was mediated through MAPK signaling (Fig. 2*A* and *B*). Notably, combination treatment resulted in stronger suppression on MAPK activation and abolished AKT activation completely, which is in agreement with its profound inhibitory effect on both EGFR and ErbB2 activation.

AG1478 + AG879 sensitizes GEO cells to apoptosis. Next, we characterized the apoptotic profiles generated by AG1478 and AG879 in quiescent GEO cells. Using similar concentrations of AG1478 and AG879 as above, significant PARP cleavage was observed with the combination treatment of 5 μmol/L AG1478 and 1 μmol/L AG879 but not with single inhibitor treatments (Fig. 3*A*). This observation indicated that GEO cells were resistant to single EGFR or ErbB2 TKIs for apoptosis induction but were sensitive to blockade of both EGFR and ErbB2 phosphorylation. This also confirms our hypothesis that both EGFR and ErbB2 are essential for GEO cell proliferation as well as cell survival. To further quantitate apoptosis, a cell death detection ELISA was used for quantification of DNA fragmentation, a hallmark for apoptosis. After 72 hours of treatment with the same combination regimen in subconfluent GEO cells, DNA fragmentation was measured as described in Materials and Methods. A more-than-additive effect of apoptosis induction by the combination treatment was observed with a 7-fold increase of DNA fragmentation compared with a 2.35- and 2.4-fold increase for AG1478 and AG879 treatment alone, respectively (Fig. 3*B*). The correlation of treatment conditions inducing PARP cleavage and DNA fragmentation with conditions inhibiting both EGFR and ErbB2 phosphorylation suggested linkage of cell survival to the ErbB signaling network. Furthermore, the failure of individual ErbB inhibitors to induce apoptosis could be explained by the failure of single inhibitors to inhibit both ErbB components (Fig. 2). This shows the rationale for targeting the two receptors simultaneously using a combination approach or a dual inhibitor of ErbB receptors.

GW572016 has higher potency for inhibition of cell proliferation and induction of apoptosis than AG1478 and AG879. GW572016 is a dual EGFR and ErbB2 TKI with equal inhibitory potency for inhibition of phosphorylation of both EGFR and ErbB2 at 10 and 9 nmol/L, respectively in cell-free systems (37). Both AG1478 and GW572016 belong to 4-anilinoquinazoline

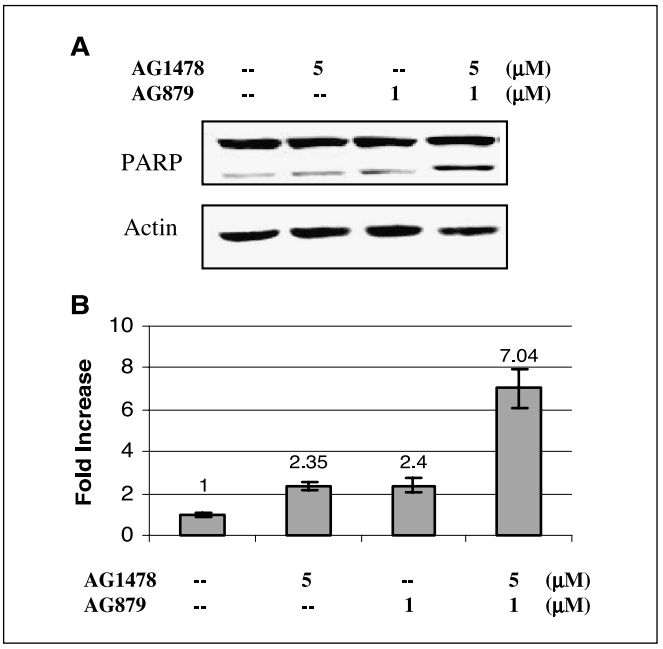

Figure 3. Effect of AG1478 + AG879 on induction of apoptosis. *A,* Western blot analysis of PARP cleavage. Quiescent GEO cells were pretreated with AG1478, AG879, and AG1478 + AG879 at the indicated concentrations for 6 hours. Cells were then released in fresh supplemented medium containing 0.1% DMSO or various concentrations of drugs for 24 hours as indicated. Whole cell lysates were subjected to SDS-PAGE analysis and probed with a specific anti-PARP antibody. Actin was used as a loading control. *B,* DNA-histone nucleosome release ELISA. Quantitation of DNA fragmentation in GEO cells was determined after 72 hours of drug treatment using the Cell Death Detection ELISA Plus kit as described in Materials and Methods. Absorbance of DNA fragmentation was normalized with absorbance of MTT assay at the identical treatment conditions. Fold increases of DNA fragmentation were compared between control and treatment as shown in the graph. Similar experiments were repeated at least twice. Representative data. *Bars,* SD.

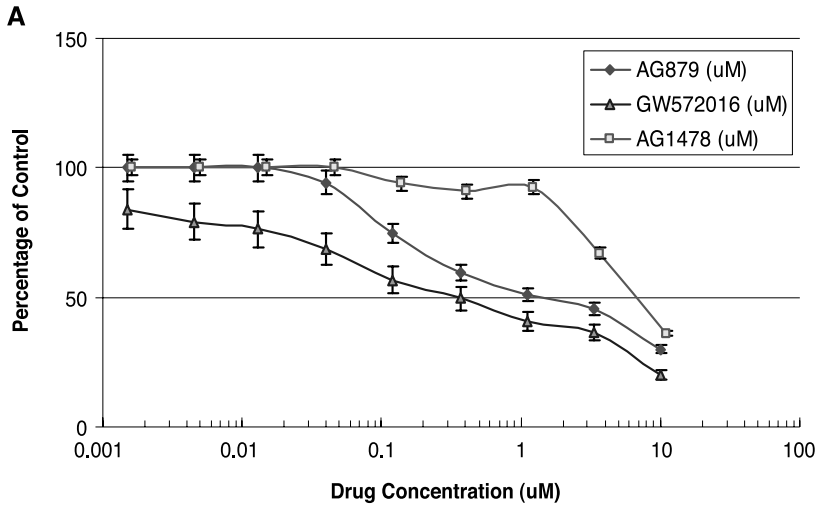

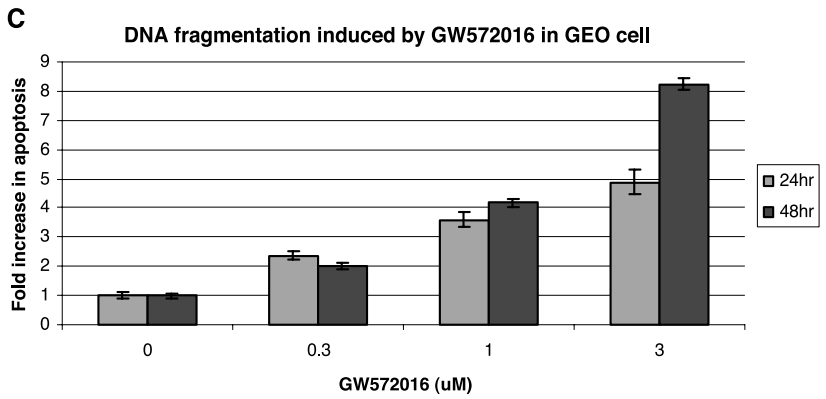

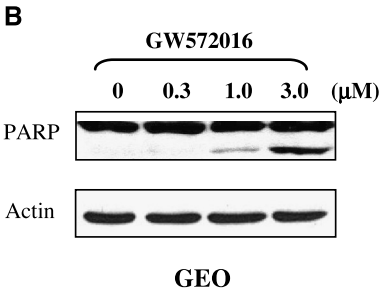

Figure 4. Effect of GW572016 on cell proliferation and apoptosis. *A,* concentration-effect curves for AG1478, AG879, and GW572016 in GEO cells. Concentration-effect curves were generated by 72-hour MTT assay as described in Materials and Methods. The growth inhibitory effects of drugs were calculated as $A_{treated}/A_{control}$. Concentrations of drugs were plotted on a log scale. *B,* Western blot analysis of PARP cleavage. Subconfluent GEO cells were treated with DMSO (0.1%) or GW572016 at 0.3, 1, and 3 μmol/L for 48 hours in supplemented medium. Whole-cell lysates were subjected to SDS PAGE analysis and probed with specific anti-PARP antibody. Actin was used as a loading control. *C,* DNA-histone nucleosome release ELISA. Quantitation of DNA fragmentation in GEO cells was determined after 24 or 48 hours GW572016 treatment using the Cell Death Detection ELISA Plus kit as described in Materials and Methods. Absorbance of DNA fragmentation was normalized to MTT assays at the identical treatment conditions. The fold increase of DNA fragmentation was compared between control and treatment. Similar experiments were repeated at least twice. Representative data. *Bars,* SD.

derivatives. As an analogue of AG1478, equal selectivity to EGFR and ErbB2 was generated in GW572016 after modification of the quinazoline pharmacophore. Consequently, we sought confirmation of our observations regarding combination treatment effects on inhibition of cell proliferation and induction of apoptosis with this dual inhibitor. First, we compared the effect of GW572016 with AG1478 and AG879 single agents on GEO cell proliferation as shown in the dose-effect curve in Fig. 4*A*. Similarly to AG1478 and AG879, GW572016 resulted in a concentration-dependent inhibition of proliferation but with a much lower IC_{50} value of 0.3 μmol/L which is 30- and 6-fold more potent than AG1478 and AG879, respectively (Table 1). Next, we evaluated the ability of GW572016 to induce apoptosis. Subconfluent GEO cells were treated with GW572016 at 0.3, 1, and 3 μmol/L in supplemented medium without growth factors. Control GEO cells with DMSO were resistant to growth factor deprivation–induced apoptosis up to 48 hours, whereas Western blot analysis revealed a concentration-dependent appearance of the cleaved form of PARP upon GW572016 treatment (Fig. 4*B*). Similarly, DNA-histone nucleosome release ELISA was conducted for quantitation of DNA fragmentation. As shown in Fig. 4*C*, GW572016 increased DNA fragmentation in a concentration-dependent manner at both 24 and 48 hours of treatment. GW572016 induced 2- and 8-fold increases of DNA fragmentation at 0.3 μmol/L for 24 hours of treatment and 3 μmol/L for 48 hours of treatment, respectively, which is comparable with the combination treatment of AG1478 + AG879 at 5 + 1 μmol/L (Fig. 2*B*). This suggests that GW572016 is at least as effective as a combination of AG1478 and AG879 for induction of apoptosis.

GW572016 inhibits EGFR and ErbB2 phosphorylation and downstream signaling. To validate the inhibition of GW572016 on EGFR and ErbB2 kinase activities, we tested the status of EGFR and ErbB2 phosphorylation in growth factor deprived GEO cells. Subconfluent GEO cells were deprived of growth factors for 5 days to induce a G_0 quiescent state. The cells were then released from the quiescent state in supplemented medium with or without addition of GW572016. DMSO (0.1%) was used as a control for drug treatment. After 6 hours of treatment with GW572016 of 0.3, 1.0, and 3.0 μmol/L, cells were lysed and analyzed for EGFR and ErbB2 phosphorylation using specific antibodies recognizing phosphorylated EGFR Y1173 and ErbB2 Y1248. As shown in Fig. 5*A*, GW572016 inhibited both phosphorylation sites in a concentration-dependent manner. We showed above that AG1478 and AG879 single agents failed to effectively block either MAPK or AKT activation in quiescent GEO cells, whereas combination treatment suppressed both pathways (Fig. 2*B*). We next tested the effect of GW572016 on MAPK and AKT pathways. Consistent with its inhibition on EGFR and ErbB2 phosphorylation, GW572016 treatment at 0.3, 1.0, and 3.0 μmol/L resulted in a concentration-dependent inhibition of phosphorylation of both MAPK and AKT (Fig. 5*B*). The potency of GW572016 for inhibition of EGFR, ErbB2, and their downstream signaling pathways correlates with the

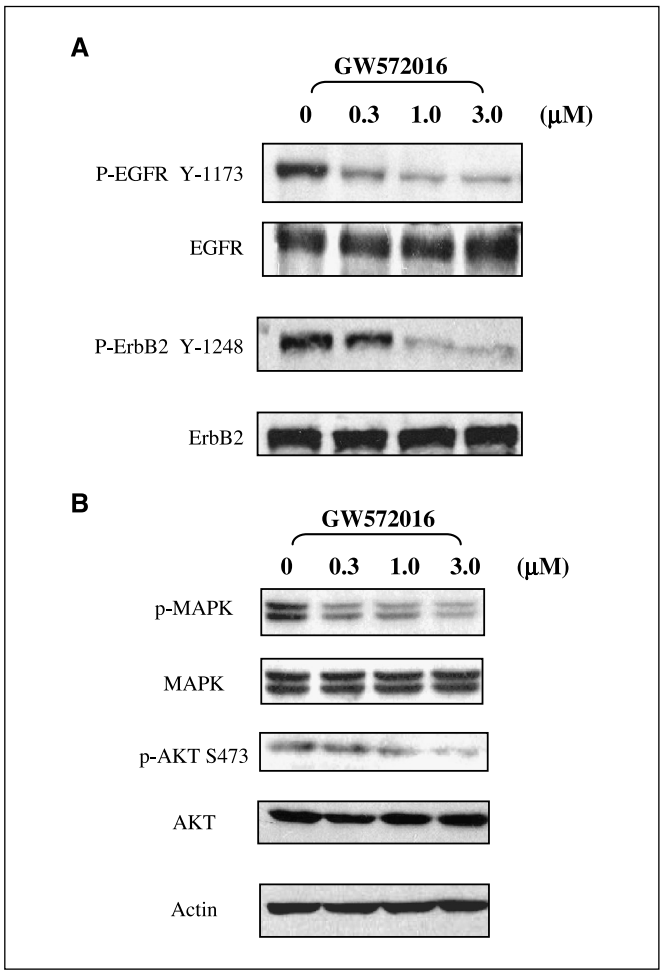

Figure 5. Western blot analysis of ErbB signaling pathway inhibition after treatment of GW572016 in GEO cells. *A,* inhibition of EGFR and ErbB2 phosphorylation. Subconfluent GEO cells were deprived of growth factors for 5 days to induce a quiescent state. Growth-arrested GEO cells were released in fresh supplemented medium containing various concentrations of GW572016 at 0.3, 1.0, and 3.0 μmol/L for 6 hours of treatment. DMSO (0.1%) was used as a control. Whole-cell lysates were subjected to SDS-PAGE analysis and probed with specific anti-phospho-EGFR Y1173 or anti-phospho-ErbB2 Y1248 antibodies. The same membranes were stripped and reblotted with total EGFR or ErbB2 antibodies as loading controls. *B,* inhibition of MAPK and AKT pathways. The same whole-cell lysates were also analyzed by Western blot using specific antibodies for phospho-MAPK and AKT. The same membranes were stripped and reblotted with total MAPK or AKT antibodies. Similar experiments were repeated at least twice. Representative data.

potency of GW572016 for induction of apoptosis. This confirms that a dual inhibitor to EGFR and ErbB2 is an effective inducer of apoptosis in conjunction with inhibition of both EGFR and ErbB2 activation.

GW572016 inhibits GEO xenograft growth. We next evaluated the *in vivo* antitumor effect of GW572016 in athymic nude mice bearing GEO tumor xenografts. For each treatment group, a total volume of 0.2 mL GEO cell suspension containing 5×10^6 cells was injected into both hind limbs of athymic nude mice. Tumors became readily apparent about 1 week after injection. GW572016 was dissolved in 0.5% hydroxypropylmethylcellulose and 0.1% Tween 80 vehicle and was given twice daily by oral gavage. The doses of GW572016 for different treatment groups were 30, 100, and 200 mg/kg, respectively. The control group of mice received hydroxypropylmethylcellulose/Tween 80 vehicle treatment at the same schedule as GW572016. Drug was administered for a total of 21 days from day 8 to day 28. As shown in Fig. 6, a concentration-dependent inhibition of GEO xenograft growth was observed. Significantly, a complete blockade of tumor growth was observed in the 200 mg/kg treatment group, which failed to sustain tumor growth during drug administration. Of note, at this dose, there was <10% weight loss in treated animals over the 21-day treatment period compared with the vehicle control group (data not shown). However, after withdrawal of drug administration, the xenografts resumed growth in all three treatment groups at a rate similar to the control group, suggesting a growth delay or static effect on tumor growth inhibition by GW572016 treatment *in vivo*.

Discussion

ErbB-targeting therapy has achieved some success in the clinical setting, especially in breast cancer patients with ErbB2 amplification and lung cancer patients with EGFR gain-of-function mutations (42, 43). However, single agent EGFR TKIs or monoclonal antibody clinical trials for colon cancer patients previously failing standard therapy have generated at best a 10% response rate despite the fact that 80% of colon cancers potentially use EGFR for pathogenesis (44, 45). The limited efficacy could arise from unblocked ErbB2 signaling in the form of EGFR/ErbB2 or ErbB2/ErbB3 heterodimers when EGFR, ErbB2, and ErbB3 coexpress in the tumor cells. For example, we recently showed that AG1478 failed to induce apoptosis at concentrations sufficient to inhibit EGFR activation in an aggressive human colon carcinoma cell line harboring constitutive expression of TGFα (46). Similarly, GEO cells were insensitive to AG1478 single-agent treatment reflected by a relatively high IC_{50} (10 μmol/L) and resistance to apoptosis induction (Fig. 3; Table 1). Interestingly, synergistic inhibition of cell proliferation and induction of apoptosis were observed in both cell models when a low AG1478 concentration was added in combination with a suboptimal dose of AG879 (1 μmol/L), indicating that the resistance to EGFR TKI could be overcome by

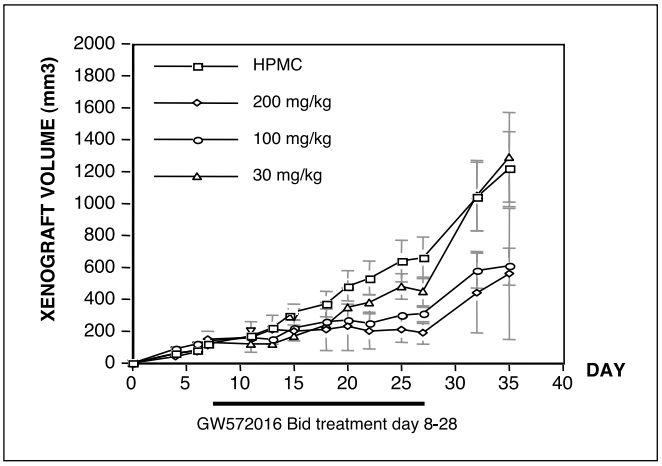

Figure 6. Effect of GW572016 on inhibition of GEO xenograft growth. A total volume of 0.2 mL GEO cell suspension containing 5×10^6 cells was injected into both hind limbs of BALB/c athymic nude mice. Starting from day 8 to day 28, mice received oral administration of GW572016 at 30, 100, and 200 mg/kg twice daily by oral gavage. Each treatment group contained eight xenografts. The control group mice received 0.5% hydroxypropylmethylcellulose (*HPMC*) and 0.1% Tween 80 vehicle treatment. Tumor volume was plotted against time. Volume (V) was determined by $V = (L \times W^2) \times 0.5$, where L is length and W is width of the tumor. Tumor volume measurement was continued after the cession of drug administration at day 28 to day 35.

a combination approach with the ErbB2 TKI. By the same token, targeting ErbB2 alone by monoclonal antibody or a TKI might not be sufficient for colon carcinoma treatment either. We have previously shown that targeting ErbB2 with a specific blocking antibody 2C4 failed to block GEO cell proliferation when EGF is present in the medium (41). More recently, a compensatory mechanism involving EGFR and ErbB2 for dimerization with ErbB3 was observed in GEO cells when ErbB2 activation was down-regulated by a specific antibody or the selective TKI AG879 (25). In this study, we confirmed our previous finding that a compensatory activation of EGFR was induced by AG879 treatment (Fig. 3*A*). It is reasonable to speculate that the resistance to AG879-induced apoptosis is linked to the compensatory activation of EGFR. Taken together, the presence of a cooperative ErbB signaling network in human colon carcinomas predetermined the failure of targeting only one component in a complicated environment of receptor complex formation.

To confirm our hypothesis that the strategy of targeting both receptors in colon carcinoma cells is superior to targeting single receptors, we compared the novel dual EGFR and ErbB2 inhibitor GW572016 with AG1478 and AG879 single agents as well as the combination of the two. To our knowledge, this is the first study to show that a dual EGFR and ErbB2 TKI is able to induce apoptosis in a human colon carcinoma cell line, which is comparable with the combination treatment of EGFR and ErbB2 TKIs. Notably, the potency of GW572016 for inhibition of GEO cell growth is 30-fold higher than AG1478 as reflected by the difference of IC_{50} values (Table 1). Intriguingly, the IC_{50} of AG1478 is decreased 10-fold in combination with AG879 in the same cell line (Table 1). The significant increase of AG1478 potency in combination with an ErbB2 inhibitor is consistent with the high potency of the single GW572016 compound because GW572016 inhibits both EGFR and ErbB2 equally. GW572016 has a similar IC_{50} for inhibiting cell proliferation in BT474 and A431 cells (37) with overexpression of ErbB2 and EGFR, respectively, and other colon carcinoma cell lines, which depend on both EGFR and ErbB2 for aberrant growth.[4] It is notable that GW572016 inhibited DNA synthesis and induced significant G_1-G_0 arrest in GEO cells similar to the cell cycle arrest effect observed in HN5 cells (data not shown). We think that the growth inhibitory effect of GW572016 in GEO cells was associated with both cell cycle arrest and apoptosis. In contrast, GW572016 has relatively low efficacy for inhibition of cell proliferation in EGFR and ErbB2 nonoverexpressing breast cancer cell lines, such as MCF-7 and T47D, with an IC_{50} that is about 20-fold higher than in these sensitive cell lines (37, 47). The sensitivity of different cell lines to GW572016 seems to be determined by the dependence on EGFR receptor for mitogenesis signaling. Interestingly, a combination of GW572016 with tamoxifen synergistically enhanced cell cycle arrest in MCF-7 cells, suggesting that this cell line depends on both ErbB and estrogen signaling for optimal growth (47). Importantly, GW572016 achieved higher efficacy than single reversible EGFR TKIs ZD1839 (Iressa, gifitinib) and OSI-774 (Tarceva) in most of the cell lines tested regardless of expression level of EGFR and ErbB2, further supporting the hypothesis that a dual TKI is superior to single agents (37, 48).

We previously showed that both MAPK and AKT pathways contributed to cell proliferation, whereas the AKT pathway is more critical for cell survival in GEO cells (17). It is reasonable to speculate that the induction of apoptosis by GW572016 was linked to inhibition of AKT activation rather than MAPK. Along this line, GW572016 induced both cell cycle arrest and apoptosis in BT474 cells but failed to induce apoptosis in HN5 cells (34). Interestingly, the discrepancy of induction of apoptosis by GW572016 on BT474 and HN5 was reflected by a differential inhibition on AKT phosphorylation rather than EGFR or ErbB2 phosphorylation (37, 49). Furthermore, the failure of inhibition of AKT activation by GW572016 in a breast cancer cell line could be a mechanism of resistance (50). However, the MAPK pathway seems to play a role in cell survival as well. Previously, we have shown that MAPK was activated by EGF stimulation independent of ErbB2 and ErbB3 signaling in GEO cells (41). Intriguingly, we observed that activation of EGFR under AG879 treatment significantly up-regulated the MAPK pathway in GEO cells, arguing for a role by MAPK as a signaling mediator of EGFR in blockade of apoptosis (Fig. 2). Of note, other pathways responding to the compensatory activation of EGFR in response to the down-regulation of ErbB2 phosphorylation could not be ruled out and need further exploration. In this study, the concentrations of GW572016 sufficient to induce PARP cleavage and DNA fragmentation correlated well with concentrations necessary to inhibit activation of EGFR and ErbB2 as well as the downstream MAPK and AKT pathways (Figs. 4 and 5). This study is consistent with others in that the concentrations of GW572016 sufficient to induce apoptosis are higher than the IC_{50} (37). Similar to previous findings, concentrations below the IC_{50} value have small inhibitory effects on EGFR or ErbB2 phosphorylation in GEO cells (data not shown) as well as in other cell lines (37).

The activity of GW572016 observed in cell culture was translated into a dose-dependent inhibition of tumor xenograft growth (Fig. 6). We used doses similar to the preclinical studies in breast cancer cell xenografts for GW572016 (49). Large variations of individual protein expression and response to treatment in animals were seen in this preclinical study; consequently, we did not attempt such correlations here. Although no tumor regression was observed at the concentrations tested in this study, a complete blockade of tumor xenograft growth was observed at 200 mg/kg during the 21 days of treatment (Fig. 6). Currently, GW572016 is in phase II and III clinical trials for treatment of advanced cancer patients (51) and has been associated with a favorable toxicity profile (52, 53). Recently, clinical pharmacodynamic studies based on the preclinical xenograft studies indicated that clinical response was associated with pretreatment ErbB2, MAPK expression, and activation as well as terminal deoxynucleotidyl transferase–mediated nick-end labeling (TUNEL) score (53). Synergistic effects between GW572016 and a panel of chemotherapeutic agents on growth inhibition of several tumor xenografts, including colon cancer, have been reported (54). Our data provide new evidence supporting development of this novel compound for the subgroup of colon cancer patients with tumors that are dependent upon both EGFR and ErbB2.

Acknowledgments

Received 7/18/2005; revised 9/26/2005; accepted 10/25/2005.

Grant support: NIH grants CA34432, CA54807, and CA16056.

The costs of publication of this article were defrayed in part by the payment of page charges. This article must therefore be hereby marked *advertisement* in accordance with 18 U.S.C. Section 1734 solely to indicate this fact.

We thank Karen K. Kuropatwinski for her assistance in organizing experimental supply and Drs. Rajinder Sawhney, Mary Spengler, and Gillian Howell, Ruiwen Wang, and Neka Simms for their helpful discussion.

[4] Unpublished data.

References

1. Threadgill DW, Dlugosz AA, Hansen LA, et al. Targeted disruption of mouse EGF receptor: effect of genetic background on mutant phenotype. Science 1995;269:230–4.
2. Sibilia M, Wagner EF. Strain-dependent epithelial defects in mice lacking the EGF receptor. Science 1995;269:234–8.
3. Di Fiore PP, Pierce JH, Fleming TP, et al. Overexpression of the human EGF receptor confers an EGF-dependent transformed phenotype to NIH 3T3 cells. Cell 1987;51:1063–70.
4. Hudziak RM, Schlessinger J, Ullrich A. Increased expression of the putative growth factor receptor p185HER2 causes transformation and tumorigenesis of NIH 3T3 cells. Proc Natl Acad Sci U S A 1987;84:7159–63.
5. Qian X, Dougall WC, Fei Z, Greene MI. Intermolecular association and *trans*-phosphorylation of different neu-kinase forms permit SH2-dependent signaling and oncogenic transformation. Oncogene 1995;10:211–9.
6. Kokai Y, Myers JN, Wada T, et al. Synergistic interaction of p185c-neu and the EGF receptor leads to transformation of rodent fibroblasts. Cell 1989;58:287–92.
7. Egan SE, Weinberg RA. The pathway to signal achievement. Nature 1993;365:781–3.
8. Rodrigues GA, Falasca M, Zhang Z, Ong SH, Schlessinger J. A novel positive feedback loop mediated by the docking protein Gab1 and phosphatidylinositol 3-kinase in epidermal growth factor receptor signaling. Mol Cell Biol 2000;20:1448–59.
9. Holgado-Madruga M, Emlet DR, Moscatello DK, Godwin AK, Wong AJ. A Grb2-associated docking protein in EGF- and insulin-receptor signalling. Nature 1996;379:560–4.
10. Hu P, Margolis B, Skolnik EY, et al. Interaction of phosphatidylinositol 3-kinase-associated p85 with epidermal growth factor and platelet-derived growth factor receptors. Mol Cell Biol 1992;12:981–90.
11. Salomon DS, Brandt R, Ciardiello F, Normanno N. Epidermal growth factor-related peptides and their receptors in human malignancies. Crit Rev Oncol Hematol 1995;19:183–232.
12. Zhau HE, Zhang X, von Eschenbach AC, et al. Amplification and expression of the c-erb B-2/*neu* proto-oncogene in human bladder cancer. Mol Carcinog 1990;3:254–7.
13. Kapitanovic S, Radosevic S, Kapitanovic M, et al. The expression of p185(HER-2/*neu*) correlates with the stage of disease and survival in colorectal cancer. Gastroenterology 1997;112:1103–13.
14. Slamon DJ, Godolphin W, Jones LA, et al. Studies of the HER-2/*neu* proto-oncogene in human breast and ovarian cancer. Science 1989;244:707–12.
15. Poller DN, Spendlove I, Baker C, et al. Production and characterization of a polyclonal antibody to the c-erbB-3 protein: examination of c-erbB-3 protein expression in adenocarcinomas. J Pathol 1992;168:275–80.
16. Wang D, Patil S, Li W, et al. Activation of the TGFα autocrine loop is downstream of IGF-I receptor activation during mitogenesis in growth factor dependent human colon carcinoma cells. Oncogene 2002;21:2785–96.
17. Venkateswarlu S, Dawson DM, St Clair P, et al. Autocrine heregulin generates growth factor independence and blocks apoptosis in colon cancer cells. Oncogene 2002;21:78–86.
18. Jiang D, Yang H, Willson JK, et al. Autocrine transforming growth factor α provides a growth advantage to malignant cells by facilitating re-entry into the cell cycle from suboptimal growth states. J Biol Chem 1998;273:31471–9.
19. Howell GM, Humphrey LE, Ziober BL, et al. Regulation of transforming growth factor α expression in a growth factor-independent cell line. Mol Cell Biol 1998;18:303–13.
20. Albanell J, Codony-Servat J, Rojo F, et al. Activated extracellular signal-regulated kinases: association with epidermal growth factor receptor/transforming growth factor α expression in head and neck squamous carcinoma and inhibition by anti-epidermal growth factor receptor treatments. Cancer Res 2001;61:6500–10.
21. Johnson GR, Saeki T, Gordon AW, et al. Autocrine action of amphiregulin in a colon carcinoma cell line and immunocytochemical localization of amphiregulin in human colon. J Cell Biol 1992;118:741–51.
22. Jiang D, Liang J, Humphrey LE, Yang H, Brattain MG. Expression of TGFα autocrine activity in human colon carcinoma CBS cells is autoregulated and independent of exogenous epidermal growth factor. J Cell Physiol 1998;175:174–83.
23. Awwad RA, Sergina N, Yang H, et al. The role of transforming growth factor α in determining growth factor independence. Cancer Res 2003;63:4731–8.
24. Ziober BL, Willson JK, Hymphrey LE, Childress-Fields K, Brattain MG. Autocrine transforming growth factor-α is associated with progression of transformed properties in human colon cancer cells. J Biol Chem 1993;268:691–8.
25. Hu YP, Venkateswarlu S, Sergina N, et al. Reorganization of ErbB family and cell survival signaling following knockdown of ErbB2 in colon cancer cells. J Biol Chem 2005;280:27383–92.
26. Ciardiello F, Caputo R, Troiani T, et al. Antisense oligonucleotides targeting the epidermal growth factor receptor inhibit proliferation, induce apoptosis, and cooperate with cytotoxic drugs in human cancer cell lines. Int J Cancer 2001;93:172–8.
27. Ciardiello F, Bianco R, Damiano V, et al. Antiangiogenic and antitumor activity of anti-epidermal growth factor receptor C225 monoclonal antibody in combination with vascular endothelial growth factor antisense oligonucleotide in human GEO colon cancer cells. Clin Cancer Res 2000;6:3739–47.
28. Ciardiello F, Caputo R, Bianco R, et al. Antitumor effect and potentiation of cytotoxic drugs activity in human cancer cells by ZD-1839 (Iressa), an epidermal growth factor receptor-selective tyrosine kinase inhibitor. Clin Cancer Res 2000;6:2053–63.
29. De Luca A, Selvam MP, Sandomenico C, et al. Antisense oligonucleotides directed against EGF-related growth factors enhance anti-proliferative effect of conventional anti-tumor drugs in human colon-cancer cells. Int J Cancer 1997;73:277–82.
30. Rose WC, Wild R. Therapeutic synergy of oral taxane BMS-275183 and cetuximab versus human tumor xenografts. Clin Cancer Res 2004;10:7413–7.
31. Normanno N, De Luca A, Maiello MR, et al. CRIPTO-1: a novel target for therapeutic intervention in human carcinoma. Int J Oncol 2004;25:1013–20.
32. Normanno N, Bianco C, Damiano V, et al. Growth inhibition of human colon carcinoma cells by combinations of anti-epidermal growth factor-related growth factor antisense oligonucleotides. Clin Cancer Res 1996;2:601–9.
33. Brignola PS, Lackey K, Kadwell SH, et al. Comparison of the biochemical and kinetic properties of the type 1 receptor tyrosine kinase intracellular domains. Demonstration of differential sensitivity to kinase inhibitors. J Biol Chem 2002;277:1576–85.
34. Rusnak DW, Affleck K, Cockerill SG, et al. The characterization of novel, dual ErbB-2/EGFR, tyrosine kinase inhibitors: potential therapy for cancer. Cancer Res 2001;61:7196–203.
35. Fry DW, Bridges AJ, Denny WA, et al. Specific, irreversible inactivation of the epidermal growth factor receptor and erbB2, by a new class of tyrosine kinase inhibitor. Proc Natl Acad Sci U S A 1998;95:12022–7.
36. Cockerill S, Stubberfield C, Stables J, et al. Indazolylamino quinazolines and pyridopyrimidines as inhibitors of the EGFr and C-erbB-2. Bioorg Med Chem Lett 2001;11:1401–5.
37. Rusnak DW, Lackey K, Affleck K, et al. The effects of the novel, reversible epidermal growth factor receptor/ErbB-2 tyrosine kinase inhibitor, GW2016, on the growth of human normal and tumor-derived cell lines *in vitro* and *in vivo*. Mol Cancer Ther 2001;1:85–94.
38. Taylor CW, Brattain MG, Yeoman LC. Rate of growth and extent of differentiation reflected by cytoplasmic proteins and antigens of human colon tumor cell lines. Cancer Res 1984;44:1200–5.
39. Chou TC, Talalay P. Quantitative analysis of dose-effect relationships: the combined effects of multiple drugs or enzyme inhibitors. Adv Enzyme Regul 1984;22:27–55.
40. Levitzki A, Gazit A. Tyrosine kinase inhibition: an approach to drug development. Science 1995;267:1782–8.
41. Jackson JG, St Clair P, Sliwkowski MX, Brattain MG. Blockade of epidermal growth factor- or heregulin-dependent ErbB2 activation with the anti-ErbB2 monoclonal antibody 2C4 has divergent downstream signaling and growth effects. Cancer Res 2004;64:2601–9.
42. Pao W, Miller VA. Epidermal growth factor receptor mutations, small-molecule kinase inhibitors, and non-small-cell lung cancer: current knowledge and future directions. J Clin Oncol 2005;23:2556–68.
43. Baselga J, Gianni L, Geyer C, et al. Future options with trastuzumab for primary systemic and adjuvant therapy. Semin Oncol 2004;31:51–7.
44. Normanno N, Bianco C, De Luca A, Maiello MR, Salomon DS. Target-based agents against ErbB receptors and their ligands: a novel approach to cancer treatment. Endocr Relat Cancer 2003;10:1–21.
45. Black JD, Brattain MG, Krishnamurthi SA, Dawson DM, Willson JK. ErbB family targeting. Curr Opin Investig Drugs 2003;4:1451–4.
46. Zhou Y, Brattain MG. Synergy of epidermal growth factor receptor kinase inhibitor AG1478 and ErbB2 kinase inhibitor AG879 in human colon carcinoma cells is associated with induction of apoptosis. Cancer Res 2005;65:5848–56.
47. Chu I, Blackwell K, Chen S, Slingerland J. The dual ErbB1/ErbB2 inhibitor, lapatinib (GW572016), cooperates with tamoxifen to inhibit both cell proliferation- and estrogen-dependent gene expression in antiestrogen-resistant breast cancer. Cancer Res 2005;65:18–25.
48. Liu Y, Majumder S, McCall W, et al. Inhibition of HER-2/neu kinase impairs androgen receptor recruitment to the androgen responsive enhancer. Cancer Res 2005;65:3404–9.
49. Xia W, Mullin RJ, Keith BR, et al. Anti-tumor activity of GW572016: a dual tyrosine kinase inhibitor blocks EGF activation of EGFR/erbB2 and downstream Erk1/2 and AKT pathways. Oncogene 2002;21:6255–63.
50. Zhou H, Kim YS, Peletier A, et al. Effects of the EGFR/HER2 kinase inhibitor GW572016 on. Int J Radiat Oncol Biol Phys 2004;58:344–52.
51. Lockhart C, Berlin JD. The epidermal growth factor receptor as a target for colorectal cancer therapy. Semin Oncol 2005;32:52–60.
52. Bence AK, Anderson EB, Halepota MA, et al. Phase I pharmacokinetic studies evaluating single and multiple doses of oral GW572016, a dual EGFR-ErbB2 inhibitor, in healthy subjects. Invest New Drugs 2005;23:39–49.
53. Spector NL, Xia W, Burris H III, et al. Study of the biologic effects of lapatinib, a reversible inhibitor of ErbB1 and ErbB2 tyrosine kinases, on tumor growth and survival pathways in patients with advanced malignancies. J Clin Oncol 2005;23:2502–12.
54. Mullin RJ, Murray DM, Onori JA, Keith BR. Xenograft response to combination therapy with the ErbB1-ErbB2 tyrosine kinase inhibitor GW572016. Proc AACR 2004;44:3823.

Blockade of EGFR and ErbB2 by the Novel Dual EGFR and ErbB2 Tyrosine Kinase Inhibitor GW572016 Sensitizes Human Colon Carcinoma GEO Cells to Apoptosis

Yunfei Zhou, Song Li, Yi P. Hu, et al.

Cancer Res 2006;66:404-411.